Supplemental Figure Legends

Supplemental Figure S1. Mutation and purification of BACs for pro-nuclear microinjection. (**A**) *HTT* genomic locus before manipulation by Red/ET recombination as predicted on the original mutant version of BAC clone RP11-866L6. Exon-9 containing S421 is marked in grey and flanking sequences are in black. The codon to be mutated and the insertion position of FRT-PGK-gb2-*neo/km*-FRT selection cassette are both emboldened. Locations of control primers used for PCR are also indicated. Note that S495 is equivalent to S421 of conventional HTT sequence nomenclature in the context of the expanded 97Q repeat. (**B**) *HTT* genomic locus after manipulation by Red/ET. The introduced point mutation S421A (S421D not shown) in exon-9 of *HTT* locus is shown in bold. The remaining FRT-site after removal of FRT-PGK-gb2-*neo/km*-FRT cassette is grey and emboldened. The primer binding site used for amplification of the kanamycin selection cassette is indicated in addition to the primers used for PCR. (**C**) Pulsed-field gel electrophoresis confirms that the BACs (S421A not shown) are intact and free of degraded BAC DNA fragments before pro-nuclear microinjection to generate transgenic founders.

Supplemental Figure S2. Additional biochemical characterization of mHTT levels in mHTT-S421D and mHTT-S421A mice. (**A**) Representative western blot showing expression levels of mHTT from cortical lysates of BACHD and mHTT-S421D mice. The blot was probed with mAb 1C2 and anti-γ-tubulin as a loading control. (**B**) Representative western blot demonstrating expression levels of mHTT from cortical lysates of mHTT-S421A and BACHD mice, as well as from a previously generated cortical lysate from a BACHD-L mouse. WT sample run on the same gel but noncontiguous with other depicted lanes. (**C**) Quantification of expression levels of the mHTT from cortical lysate of 2-month-old BACHD, mHTT-S421D, and mHTT-S421A mice. Values are based on the mean of three independent blots with mAb 1C2 and compared across different blots by normalization to BACHD samples. Each value was first normalized for input by using the anti-γ-tubulin control. $F=22.04$, $p<0.0001$, one-way ANOVA; S421A vs BACHD/S421D, $p<0.0001$ ****$p<0.0001$; n.s., not significant.

Supplemental Figure S3. Soluble levels of mHTT protein and cleavage into polyQ fragments do not obviously change with age in BACHD, mHTT-S421D, and mHTT-S421A mice. (**A**) Western blot of mHTT from cortical lysates of BACHD, mHTT-S421D, and mHTT-S421A mice at 1 and 12 months of age. The blot was probed with mAb 1C2 and anti-γ-tubulin as a loading control. (**B**) Overexposure of the blot depicted in (A) reveals no marked differences in the production of mHTT polyQ fragments among BACHD, mHTT-S421D, and mHTT-S421A mice at either age.

Supplemental Figure S4. mHTT-S421D mutant mice display the obesity-with-age phenotype seen in BACHD mice. Weight measurements of the cohort of BACHD (n=7), mHTT-S421D (n=17), and WT (n=31) mice prior to the initiation of behavioral testing at each time. Data were analyzed by two-way repeated measures ANOVA, followed by comparisons of the means with Bonferroni post-hoc tests. *$p<0.05$; ***$p<0.001$; ****$p<0.0001$; n.s., not significant.

Supplemental Figure S5. Additional behavioral studies. (**A**) Comparison of time spent in the center versus the periphery of the open field reveals a trend for less time spent in the center for BACHD mice (n=7) than both WT (n=31) and mHTT-S421D (n=17) mice at 12 months of age. (**B**) Comparison of percent time spent in the closed arms of the elevated plus maze does not demonstrate the normalization of mHTT-induced anxiety-like behavior in mHTT-S421D mice that was found in the light-dark box assay (see Figure 3E). (**C**) Analysis of the mean sucrose

preference over 24 hours reveals no significant phenotypic discrepancies in a second cohort of WT (*n*=22), BACHD (*n*=11), and mHTT-S421D (*n*=10) mice at 3 months of age. (**D**) Analysis of the Porsolt forced swim test reveals no significant phenotypic discrepancies in the same second cohort of mice. (**E**) Comparison of the prepulse inhibition of startle in the same second cohort of mice. Two-way repeated measures ANOVA reveals significant effects of acoustic intensity ($p<0.0001$) and genotype ($p=0.0075$) with no evidence of an interaction ($p=0.9130$). In **A**–**D**, one-way ANOVA statistical anaylsis was utilized. Bonferroni post-hoc tests used for all pair-wise comparison. **$p<0.01$.

Supplemental Figure S6. Effect of S421 mutation on striatal and cortical histopathology caused by expression of mHTT at 12 months of age. (**A**) Representative brain slice depicting NeuN staining at low magnification to illustrate the striatal boundaries used for stereological measurements. The scale bar represents 200 µm. (**B**) Measurement of cortical volume of BACHD (*n*=6), mHTT-S421D (*n*=7), and WT (*n*=6) mice by unbiased stereology. (**C**) Measurement of cortical NeuN counts with correction for volume changes in the same cohort. In **B** and **C**, one-way ANOVA statistical analysis was utilized with Bonferroni post-hoc tests for all pair-wise comparisons without detection of statistically significant differences.

Supplemental Figure S7. Equivalent m*HTT* mRNA levels in cerebellum and brain stem of BACHD and mHTT-S421D mice. Quantification of the levels of cerebellar **(A)** and brain stem **(B)** m*HTT* transcript in BACHD and mHTT-S421D mice by qRT-PCR. The results are from four independent samples per transgenic line, each run in quadruplicate. Values were normalized to BACHD samples and means were compared with an unpaired t-test. n.s., not significant.

Table S1. Summary statistics for rotarod post-hoc analysis			
Comparison	**3 months**	**6 months**	**12 months**
mHTT-S421D vs WT	$t = 2.108$, $p > 0.05$	$t = 1.767$, $p > 0.05$	$t = 3.328$ $p < 0.01$
mHTT-S421D vs BACHD	$t = 3.180$, $p < 0.05$	$t = 3.995$, $p < 0.001$	$t = 4.160$, $p < 0.001$
BACHD vs WT	$t = 4.933$, $p < 0.0001$	$t = 5.561$, $p < 0.0001$	$t = 6.865$, $p < 0.0001$

Table S2. Potential polyQ disease-associated protein Akt phosphorylation sites

Site	Score[A]	Percentile[A]	Sequence	Evidence for phosphorylation[B]
huntingtin (P42858)				
S421	0.3742	0.03%	GGRSRSG**S**IVELIAG	yes
T2068	0.4476	0.10%	LDRFRLS**T**MQDSLSP	no
T1024	0.4817	0.18%	TSTTRAL**T**FGCCEAL	no
S2059	0.5648	0.64%	QRHQRLY**S**LLDRFRL	no
S2550	0.5951	0.98%	TRFGRKL**S**IIRGIVE	no
S2116	0.5982	1.02%	QCWTRSD**S**ALLEGAE	no
T2457	0.6229	1.39%	EFIYRIN**T**LGWTSRT	no
S419	0.6477	1.87%	ESGGRSR**S**GSIVELI	yes
S883	0.654	2.02%	EIDFRLV**S**FLEAKAE	no
S1826	0.6564	2.08%	SLNLRAR**S**MITTHPA	no
S1349	0.6657	2.32%	GRAQRLG**S**SSVRPGL	no
T1798	0.6834	2.83%	SGMFRRI**T**AAATRLF	no
T800	0.6863	2.92%	MGTIRTL**T**GNTFSLA	no
S1228	0.6893	3.02%	VTTSKSS**S**LGSFYHL	no
T1065	0.698	3.31%	DESRKSC**T**VGMATMI	no
T2174	0.7009	3.41%	FEAAREV**T**LARVSGT	no
S623	0.7061	3.60%	SEAFRNS**S**MALQQAH	no
S1702	0.7182	4.10%	LSRIQEL**S**FSPYLIS	no
S1864	0.7223	4.29%	QQTPKRH**S**LSSTKLL	yes
T2337	0.7241	4.38%	SPERRTN**T**PKAISEE	no
S691	0.7329	4.80%	VHCVRLL**S**ASFLLTG	no
T3133	0.6891	3.01%	SPYHRLL**T**CLRNVHK	no
ataxin-1 (P54253)				
S775	0.4009	0.05%	ATRKRRW**S**APESRKL	yes
S262	0.6229	1.39%	QNTGRTA**S**PPAIPVH	no
T282	0.681	2.76%	TMIPHTL**T**LGPPSQV	no
T32	0.7073	3.65%	SSEEKAP**T**LPSDNHR	no
S406	0.7236	4.35%	QATHREA**S**PSTLNDK	yes
ataxin-2 (Q99700)				
S697	0.5486	0.50%	PRSPRQN**S**IGNTPSG	no
S530	0.5732	0.72%	SMPSRST**S**HTSDFNP	yes
S927	0.5916	0.93%	EFNPRSF**S**QPKPSTT	no
T913	0.6236	1.40%	AEQVRKS**T**LNPNAKE	no
S617	0.6421	1.74%	TMPKRMS**S**EGPPRMS	no
T580	0.67	2.44%	SLPPRAA**T**PTRPPSR	yes

T741	0.683	2.82%	PASNRAV**T**PSSEAKD	yes
S69	0.6852	2.89%	PPPSRQS**S**PPSASDC	no
S597	0.7032	3.50%	SRPSRPP**S**HPSAHGS	no
T532	0.7089	3.71%	PSRSTSH**T**SDFNPNS	no
S569	0.7156	3.99%	RPPSRYQ**S**GPNSLPP	no
S637	0.734	4.86%	HPRNHRV**S**AGRGSIS	yes
T423	0.7367	4.99%	DSSLSSY**T**VPLERDN	no

ataxin-3 (P54252)

S265	0.698	3.31%	QGSSRNI**S**QDMTQTS	yes
S321	0.7189	4.13%	QQQQRDL**S**GQSSHPC	no

voltage-dependent P/Q-type calcium channel subunit alpha-1A (O00555)[c]

S984	0.5224	0.33%	RARHREG**S**RPARGGE	no
S2093	0.5805	0.80%	EGQGRAA**S**MPRLPAE	no
S2127	0.6037	1.09%	SPMKRSA**S**VLGPKAR	no
T58	0.6142	1.25%	SMAQRAR**T**MALYNPI	no
S875	0.6178	1.31%	RARDPSG**S**AGLDARR	no
S2167	0.6247	1.42%	SHRASER**S**LGRYTDV	no
S2160	0.6346	1.59%	HQRRRDR**S**HRASERS	no
S1822	0.6437	1.78%	EYLTRDS**S**ILGPHHL	no
S2251	0.6439	1.79%	QRWSRSP**S**EGREHMA	yes
S873	0.6456	1.82%	HDRARDP**S**GSAGLDA	no
S2265	0.6571	2.10%	AHRQGSS**S**VSGSPAP	yes
T2045	0.6613	2.21%	EMFQKTG**T**WSPEQGP	no
S910	0.6683	2.39%	DHHAREG**S**LEQPGFW	yes
T1684	0.6723	2.51%	TIRILLW**T**FVQSFKA	no
T73	0.6893	3.02%	PVRQNCL**T**VNRSLFL	no
S947	0.6933	3.15%	SRESRSG**S**PRTGADG	no
T2334	0.7072	3.65%	ARPGRAA**T**SGPRRYP	no
S1860	0.712	3.84%	YQMLRHM**S**PPLGLGK	no
S2140	0.7184	4.11%	ARRLDDY**S**LERVPPE	no
S606	0.7293	4.63%	SLRNLVV**S**LLNSMKS	no
S2247	0.7333	4.82%	RARDQRW**S**RSPSEGR	no
S2443	0.7347	4.89%	PPPVRHA**S**SGATGRS	no
S2457	0.7335	4.83%	SPRTPRA**S**GPACASP	no

ataxin-7 (O15265)

S583	0.4858	0.19%	RIPHRTN**S**VPTSQCG	no
S710	0.6072	1.14%	SGKKRKN**S**SPLLVHS	no
S208	0.6236	1.40%	SGSNRSS**S**GGVLSAS	no

S171	0.6444	1.80%	SHYERRH**S**SSSKPPL	no
S686	0.6555	2.06%	SLRPKES**S**GNSTNCQ	no
S647	0.6933	3.15%	SMQSRQV**S**SSSSSPS	no
S368	0.7027	3.48%	SLTCKTH**S**LTQRRAV	no
S492	0.7042	3.53%	EPASRLS**S**EEGEGDD	no
S361	0.7095	3.74%	TKKPCTR**S**LTCKTHS	no
S649	0.7153	3.98%	QSRQVSS**S**SSSPSTP	no
S451	0.7217	4.26%	KPKPHTP**S**LPRPPGC	no
S172	0.7361	4.96%	HYERRHS**S**SSKPPLA	no
S840	0.6812	2.77%	IGKKRKC**S**PSSSSIN	yes

TATA-box-binding protein (P20226)

T210	0.7142	3.93%	RIREPRT**T**ALIFSSG	no

atrophin-1 (P54259)

T664	0.5701	0.69%	PPSFRTG**T**PPGYRGT	no
S672	0.6641	2.28%	PPGYRGT**S**PPAGPGT	no
S132	0.6753	2.60%	DQDNRST**S**PSIYSPG	no
S182	0.6891	3.01%	TPRQPEA**S**FEPHPSV	no
S640	0.6948	3.20%	PYGKRAP**S**PGAYKTA	no
T686	0.7141	3.93%	TFKPGSP**T**VGPGPLP	no
S882	0.7194	4.16%	TPALRTL**S**EYARPHV	no
S101	0.7214	4.25%	QELPRPQ**S**PSDLDSL	yes
S134	0.7286	4.60%	DNRSTSP**S**IYSPGSV	no
S9	0.7329	4.80%	KTRQNKD**S**MSMRSGR	yes
S891	0.7369	5.00%	YARPHVM**S**PGNRNHP	no
S1124	0.6647	2.29%	PYRDLPA**S**LSAPMSA	no

androgen receptor (P10275)

S213	0.5741	0.73%	SGRAREA**S**GAPTSSK	yes
T755	0.728	4.56%	AMGWRSF**T**NVNSRML	no
S791	0.6432	1.77%	CVRMRHL**S**QEFGWLQ	yes

All results from Scansite (www.scansite.mit.edu) as of 04/04/2013.

Swiss-Prot accession number for protein follows name in parentheses.

[A]Scores in Scansite start at 0.000 if the sequence optimally matches the given motif, and the scores increase for sequences as they diverge from the optimal match. The score percentile reflects how good a score is for a given motif.

[B]Evidence for phosphorylation refers to the presence or absence of a phosphorylation site documented at PhosphoSite (www.phosphosite.org) as of 04/04/2013.

[C]However, see Du et al. (*Cell* 154:118–133, 2013) for an alternative mechanism of neurodegeneration in SCA6.

Supplemental Methods

BAC recombineering. S421A/D point mutations were inserted into the original BAC vector used to make BACHD mice (41) by one Red/ET triple recombination step (Gene Bridges GmbH). PCR was used to amplify a DNA fragment carrying the respective point mutation, as well as a stretch of homology to an FRT-flanked selection marker cassette that was generated by an independent PCR. Red/ET recombination of these two products and the original *HTT** BAC yielded BAC-*HTT**S421A/D-FRT-PGK-gb2-*neo/km*-FRT as confirmed by subsequent PCR and sequencing. An FLP-recombination step was then performed to remove the selectable marker, leaving only an FRT-site as a footprint in the adjacent intron approximately 400 nt 3′ of the modified exon. Finally, correct removal of the selection marker with preservation of the point mutation was verified by PCR and sequencing of regions around the point of mutation, exon-1, and the native stop codon.

Generation and breeding of transgenic mice. The final modified, sequence-confirmed BACs were prepared as described (82) and confirmed to be free of degraded DNA by pulsed-field gel electrophoresis. BAC DNA was linearized overnight with PI-Sce I at 37°C, dialyzed into microinjection buffer, and microinjected into FvB/N pro-nuclei by the Gladstone Transgenic Core. All mice were maintained on the FvB/NJ background.

Genotyping and sequencing. Routine genotyping of BACHD, mHTT-S421D, and mHTT-S421A mice was performed as described (15). For sequencing of the region around S421, tail DNA was purified using the DNeasy Blood and Tissue kit (Qiagen). PCR was performed with the HotStar HiFidelity Polymerase Kit (Qiagen) according to the manufacturer's instructions using the following primers with an annealing temperature of 57°C: 5′-CGA GCT TCT GCA AAC CCT GAC-3′ and 5′-TTG GCA AGG AAG ATG GAA TGC AG-3′. The PCR product was purified using the DNA Clean & Concentrator Kit (Zymo Research) and submitted for sequencing (Elim Biopharmaceuticals).

Preparation of brain lysate and western blotting. Mouse brains were dissected on ice, snap-frozen on dry ice, and stored at -80°C until further use. Brains were homogenized in a modified RIPA buffer (41), supplemented with Halt Protease and Phosphatase Inhibitor Cocktails (Thermo Sci), using a pellet pestle (Kontes). The samples were then centrifuged at 4°C for 15 minutes at 13,000 rpm. The soluble supernatants were retained, and protein concentrations were determined using the BCA Protein Assay (Thermo Sci).

For western blots, NuPAGE (Invitrogen) 3-8% Tris-Acetate or 4-12% Bis-Tris pre-cast gels were used. Samples (40 μg) were prepared and run according to the manufacturer's instructions. Protein was wet-transferred overnight onto Immobilon-FL (Millipore) PVDF using NuPAGE transfer buffer with no added methanol. Immunoblots were probed with 4H7H7 (1:5000), 1C2, (Millipore, MAB1574, 1:3000), anti-HTT 2166 (Millipore, mAb2166, 1:3000), or anti-γ-tubulin (Sigma, T6557, 1:20,000). Appropriate IRDye secondary antibodies (LI-COR Biosci) were used at a 1:20,000 dilution. Images were captured with the Odyssey CLx (LI-COR Biosci).

Preparation of RNA extracts and qRT-PCR. Mice were maintained undisturbed in their home cage until immediately prior to extraction. They were subsequently anesthetized to a surgical plane of anaesthesia with isoflurane and decapitated with a sharp pair of scissors. Brains were then removed, dissected on ice, snap-frozen with liquid nitrogen, and stored at -80°C until further processing. RNA was isolated and purified with the miRNeasy Mini kit (Qiagen) according to the manufacturer's instructions, with frozen tissue being disrupted and homogenized with the TissueLyser II (Qiagen).

300 ng of RNA was converted to cDNA using the Taqman Reverse Transcription kit (Invitrogen) using a 1:1 mix of random hexamers and oligo dT(16). qRT-PCR with Sybr Green

(Applied Biosystems) was performed on 1:40 dilutions of the samples using a 7900HT Fast Real-Time PCR system (Applied Biosystems). We generated primers that anneal specifically to human *HTT* mRNA using QuantPrime (83) [forward, 5′-ATC CCG GTC ATC AGC GAC TAT C-3′; reverse, 5′-GCT TGT AAT GTT CAC GCA GTG G-3′]. Samples were normalized using primers for mouse beta-actin (QuantiTect primers, Qiagen). The standard curve method was used to analyze the data.

Behavioral testing. All testing was performed during the light phase of the light cycle, and animals were given at least 45 minutes to acclimate to the testing room. Approximately equal numbers of males and females were used per each genotype. Data were collected and scored blind to genotype. All apparatuses were cleaned with 70% ethanol between each run.

Accelerating rotarod. Motor performance was examined with an accelerating rotarod (Med Associates) in a cohort of BACHD, mHTT-S421D, and WT mice and a cohort of mHTT-S421A and WT mice at 3, 6, and 12 months of age. Mice were first trained on the rotarod at 16 rpm for three trials. The subsequent 2 days, mice were tested twice a day, three times each session, as it accelerated from 4 to 40 rpm over 5 minutes. Only mice with data collected at each time point were analyzed.

Open-field. Total activity and rearing activity was assessed in an automated clear plastic chamber (41x41x30 cm) Flex-Field/Open-Field Photobeam Activity System (San Diego Instruments). Mice were placed in open-field chambers with two 16×16 photobeam arrays to detect horizontal and vertical movements. Total beam breaks and number of rears (the number of times the mouse stood erect on its hindlegs) were measured automatically by the instrument over 10 minutes.

Gait assessment. The CatWalk XT (Noldus) was used to automatically assess the mean hindlimb gait. Mice were placed on the apparatus and were removed after three runs that were judged compliant by the software (version 9.1) with its default settings. Paw identification was performed automatically by the software with human review of each call to confirm accuracy.

Light-dark box. Anxiety-like behavior was assessed in a light-dark box created with the open-field chamber described previously with the dark box insert (San Diego Instruments catalog #7001-0364) added. This insert encloses half of the chamber in darkness with a small opening allowing free passage of the mouse between the light and dark sides. During the 10-minute test, the amount of time spent in each chamber by a mouse was measured automatically by the instrument. The test was conducted under standard lighting conditions.

Elevated plus maze (EPM). Anxiety-like behavior was assessed in an EPM, which consists of two open (without walls) and two enclosed (with walls) arms elevated 63 cm above the ground (Hamilton-Kinder, Poway, CA). The test was performed under dim lighting conditions. Mice were placed at the junction between the open and closed arms of the plus maze and allowed to explore for 10 minutes. Total distance traveled and time spent in the open and closed arms were calculated based on infrared photobeam breaks.

Sucrose preference test (SPT). Anhedonia was assessed in the SPT. Mice were single housed at least 24 hours before testing and habituated to drinking water from two bottles placed in the top of their cage. Pre-weighed bottles, one containing normal drinking water and one containing 2% sucrose solution, were placed into the cage the morning of the first day of testing. Bottle placement was counter balanced across subjects to avoid drinking place preference confounds. Both the plain drinking water bottle and sucrose bottle were weighed twice daily as close to the beginning and end of the 12-hour light cycle as possible for 3 days. Percentage of sucrose intake was calculated by the following equation: % sucrose preference = (sucrose intake / (sucrose intake + H_2O intake)) X100.

Porsolt forced swim test (FST). Behavioral despair was assessed using the FST. A clear plastic cylinder 45 cm high and 20 cm in diameter was filled 2/3 of the way full with water at 20-21° C. Mice were individually placed in the cylinder and allowed to swim for 6 minutes while being video recorded. Mice were scored for immobility during the last 4 minutes of the test.

Pre-pulse Inhibition of startle test (PPI). Sensorimotor gating was assessed using the PPI. Testing was performed in a small isolated chamber (9.5x11x6 in), free from external movement and noise (Kinder Scientific). Mice were given 5 minutes to acclimate to the restraining chamber and 70dB background noise before stimulus testing began. Mice were then exposed to a series of acoustic pulses for 20 minutes in which some pulses were preceded by a weaker acoustic signal (pre-pulse) or no stimulus at all at random intervals for a total of 80 trials (23 40ms120dB trials, 14 each of the 4dbpp40ms120dB, 12dbpp40ms120dB, 20dbpp40ms120dB, and no stim trials). Average and maximum amplitudes of pulses (and those with preceding pre-pulses) were measured automatically by the device for each mouse.

Immunohistochemistry and stereology. Avertin was used to bring mice to a surgical plane of anesthesia, at which point they were perfused with saline using an automated pump. The right hemibrain was immersion-fixed in 4% paraformaldehyde in PBS at 4° for 48 hours. The volume of the neocortex was estimated in sagital brain sections sectioned with the vibratome at 50 µm, as described (84, 85). Briefly, sections were analyzed at 63× using a digital Olympus BX51 microscope and a Stereo Investigator system (MBF Biosciences, Williston, VT). Volume was estimated by point counting using Cavalieri's method. For neuron counts, the total number of NeuN-positive cells was averaged and expressed as relative numbers per area after accounting for any changes in volume.

Immunohistochemical staining of mHTT IBs. Multiple perfusion-fixed brains were embedded in gelatin blocks, post-fixed, and freeze-cut into coronal 35µm sections in 24 sequential series (NeuroScience Associates). These were stored at -20°C in cryoprotectant as individual series of sections and stained for mutant HTT-derived aggregates with an affinity purified preparation of the sheep anti-HTT antibody S830 (30 ng/mL) under uniform modified free-floating conditions (86). Binding was visualized using ultra-sensitive HRP-based Ni++/DAB immunohistochemistry. Images were collected on a Spot Slider camera on a Leica DMR microscope under the control of Image Pro Plus (Media Cybernetics), and minimal manipulations of images were performed in Adobe Photoshop CS12.0. Each field is 600x600 µm.

Analysis of HTT steady-state levels and clearance. HTT-N480-17Q constructs (19) were cotransfected with Lipofectamine 2000 (Invitrogen) into St14A cells along with myc-actin to control for transfection efficiency. When indicated, cells were treated for 4 hours with DMSO or 100 nM epoxomicin in DMSO or for 16 hours with water or 20 nM ammonium chloride/100 µM leupeptin in water. The short incubation time for epoxomicin treatment was used to eliminate the possibility of non-specific effects of epoxomicin on the lysosome. Cell culture, lysis, and western analysis were performed as described (16) with slight modifications as follows. NuPAGE Novex 4-12% Bis-Tris pre-cast gels with MOPS running buffer (Invitrogen) were used with 20 µg of sonicated whole-cell lysate. Quantitative densiometric analysis was performed on digitalized images of immunoblots using ImageJ. Water and DMSO control condition measurements were found to have no statistically significant differences and were combined for the remainder of the statistical analyses.

Huntingtin co-immunoprecipitation. St14A cells were transiently transfected as described above with the addition of HA-ubiquitin plasmid. Immunoprecipitation as previously described (73) with the following modifications and brief summary: cells were treated for 4 hours with epoxomicin (100 nM) and 1 hour with PR619 (100 µM) prior to lysis. 20 µg of the lysate was set aside for whole-cell controls. 400 µg of the lysate was diluted into 500 µL of IP buffer and combined with 1 µL of rabbit polyclonal anti-HA H6908 (Sigma) and 30 µL of Dynabeads (ThermoFisher) and rotated at 4°C overnight. After washing and elution, the eluted lysate was run on gels as described above and immunoblotted with rabbit polyclonal anti-HTT VB3130 (Viva Bioscience). Quantification was performed as above and expressed as a ratio of

immunoprecipitated to whole-cell levels per construct. Final data represent two independent experiments each run in triplicate.

Statistics. All quantified data are presented as the mean ± SEM. For all statistical analysis, Prism 5 software (GraphPad Software) was used with a significance level set at 0.05. For group comparisons, one- or two-way ANOVAs were performed as indicated with Bonferroni post-hoc analysis for pairwise comparisons unless otherwise stated. When appropriate, means of two groups were compared with an unpaired two-way t test.

Study approval. All mice were bred and maintained under standard conditions consistent with National Institutes of Health guidelines and approved by the UCSF Institutional Animal Care and Use Committee.

Kratter, *et al*, Supplemental Figure 1

A

Exon 9

ACCTGTGTTTCTCTGTTTCTAGGTTTATGAACTGACGTTACATCATACACAGCACCAAGACCACAATGTTGTGACCGGAG
CCCTGGAGCTGTTGCAGCAGCTCTTCAGAACGCCTCCACCCGAGCTTCTGCAAACCCTGACCGCAGTCGGGGGCATTGGG

S495A: change AGT to GCT
S495D: change AGT to GAT

CAGCTCACCGCTGCTAAGGAGGAGTCTGGTGGCCGAAGCCGTAGTGGG**AGT**ATTGTGGAACTTATAGGCAAGTTATTAGC
AAGGTCTACTCTTACAATTAACTTTGCAGTAATACTAGTTACACTCTATTGATTATGGGCCTGCCCTGTGCTAAGCAGTC
TGCATTCCATCTTCCTTGCCAAAACTTATAATACAAATTTCATCTTTATTTTATAAATAGGGGAGTTGGGCTGGGTGTGG

P169-check3

TGGCTCACGCCTGTAATTTCAGCACTTTGGAAGGATCGCTTCAGCCCAGGAGTTTGAGACAACCTGGCCAAGTGAGACCC

P169-check4

TGTCTCTACAAAAAAAAAAAAAAAAAAAAAAATTAGCTGGGCATGGTGGCACATGCCTGTAGTCCCAGCTGCTTTGGAGGC

Insert FRT-neo-FRT

TGAGGTGGTAGGATTGCTTAAGCCCAAGAGGTTGA**GG**CTGCAGTGAATCTTGATGGCAGCTGCACTGAGCCTGGTGACAG
AGCAAGATGCTGTCTCAAAATAAATTTAAAAATAAAATAAGAGAATTAAAGTTTAGCAGGTTGGGTGGCAAAATGAGGCC

B

Exon 9

ACCTGTGTTTCTCTGTTTCTAGGTTTATGAACTGACGTTACATCATACACAGCACCAAGACCACAATGTTGTGACCGGAG
CCCTGGAGCTGTTGCAGCAGCTCTTCAGAACGCCTCCACCCGAGCTTCTGCAAACCCTGACCGCAGTCGGGGGCATTGGG
CAGCTCACCGCTGCTAAGGAGGAGTCTGGTGGCCGAAGCCGTAGTGGG**GCT**ATTGTGGAACTTATAGGCAAGTTATTAGC
AAGGTCTACTCTTACAATTAACTTTGCAGTAATACTAGTTACACTCTATTGATTATGGGCCTGCCCTGTGCTAAGCAGTC
TGCATTCCATCTTCCTTGCCAAAACTTATAATACAAATTTCATCTTTATTTTATAAATAGGGGAGTTGGGCTGGGTGTGG

P169-check3

TGGCTCACGCCTGTAATTTCAGCACTTTGGAAGGATCGCTTCAGCCCAGGAGTTTGAGACAACCTGGCCAAGTGAGACCC

P169-check4

TGTCTCTACAAAAAAAAAAAAAAAAAAAAAAATTAGCTGGGCATGGTGGCACATGCCTGTAGTCCCAGCTGCTTTGGAGGC

FRT Foot Print — Primer Binding Site

TGAGGTGGTAGGATTGCTTAAGCCCAAGAGGTTGAG**GAAGTTCCTATTCTCTAGAAAGTATAGGAACTTC**CTCGAGCCCT
ATAGTGAGTCGTATTAGCTGCAGTGAATCTTGATGGCAGCTGCACTGAGCCTGGTGACAGAGCAAGATGCTGTCTCAAAA
TAAATTTAAAAATAAAATAAGAGAATTAAAGTTTAGCAGGTTGGGTGGCAAAATGAGGCCACACATTTAAAGCCCCTCCT

C

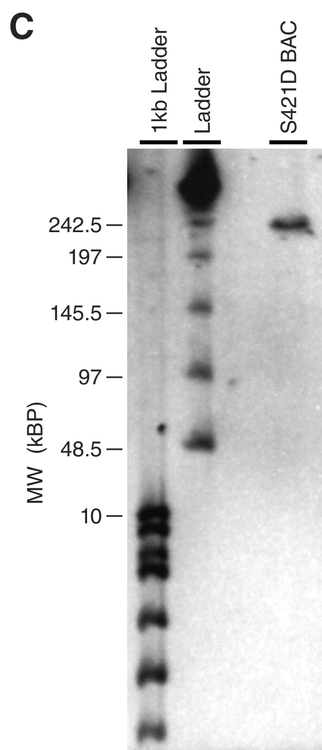

Kratter, *et al*, Supplemental Figure 2

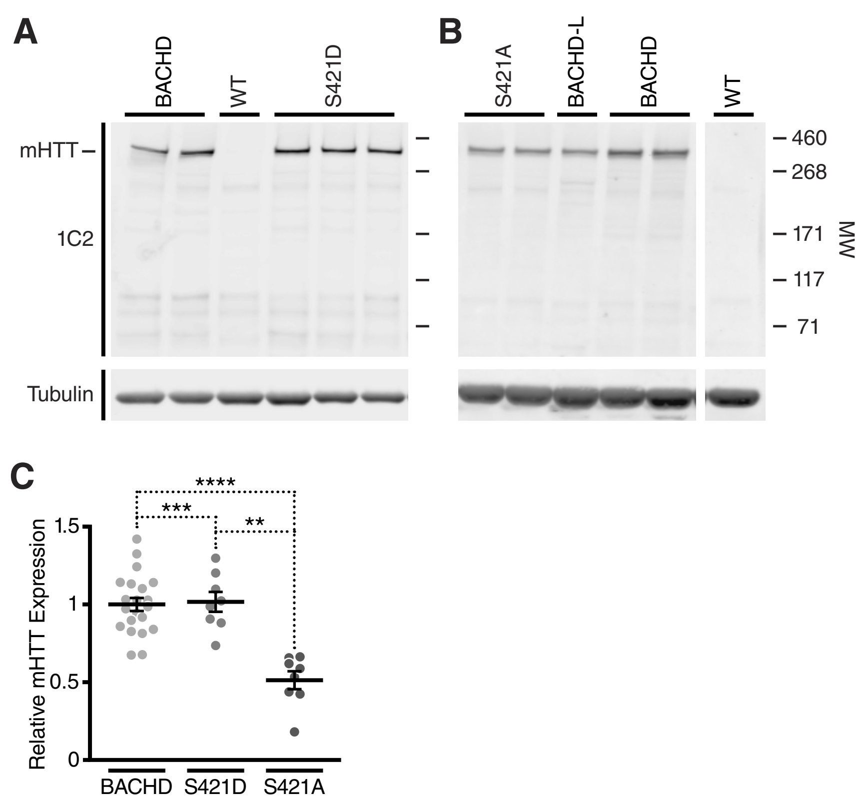

Kratter, *et al*, Supplemental Figure 3

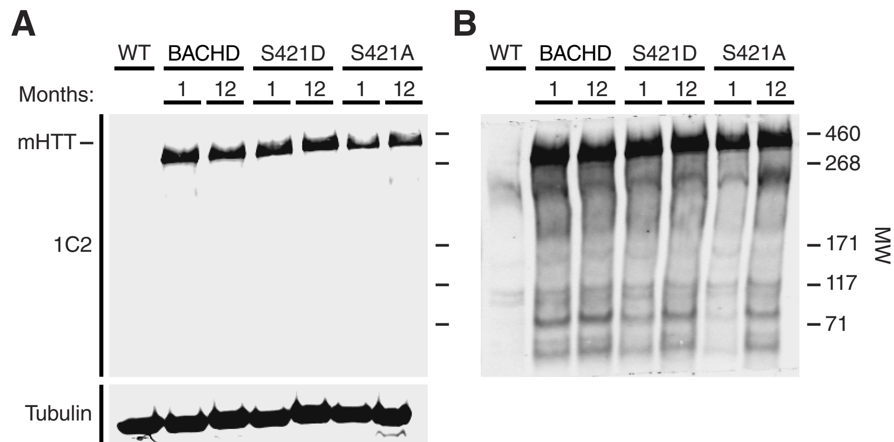

Kratter, *et al*, Supplemental Figure 4

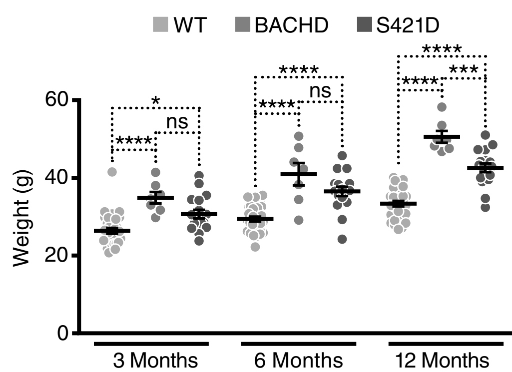

Kratter, *et al*, Supplemental Figure 5

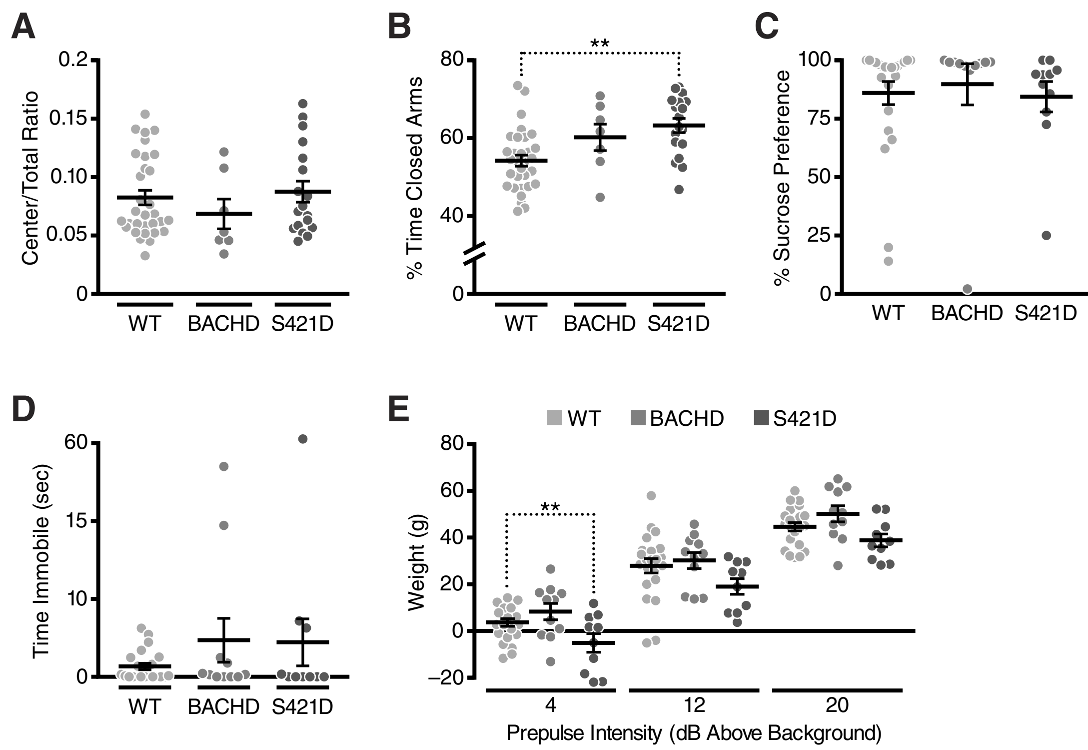

Kratter, *et al*, Supplemental Figure 6

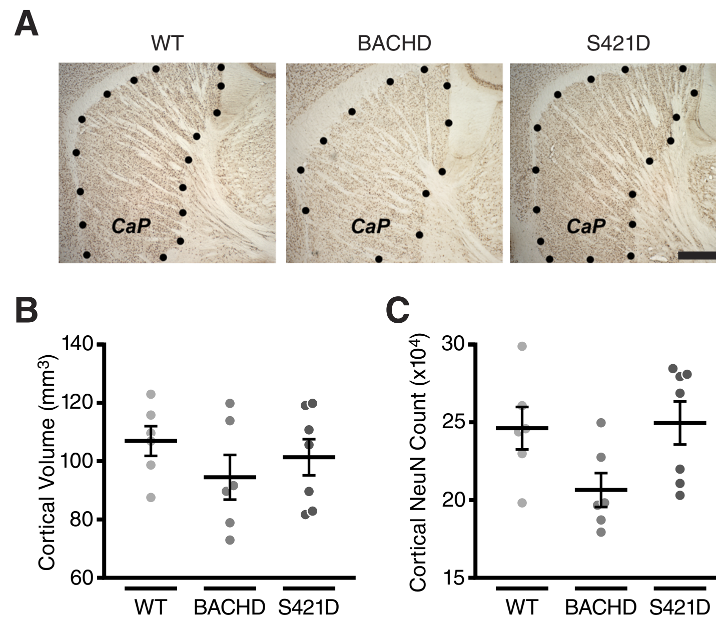

Kratter, *et al*, Supplemental Figure 7